Astronomical and Astrophysical Transactions (*AApTr*), 2016, Vol. 29, Issue 3, pp. 265–276,
ISSN 1055-6796, Photocopying permitted by license only, ©Cambridge Scientific Publishers

The influence of the kinematic effects in dark matter on the formation of population of dark halos

E.P. Kurbatov*

Institute of Astronomy, Russian Academy of Sciences, 48 Pyatnitskaya St., Moscow, 119017, Russian Federation

Received 15 September, 2015

The ΛCDM-model predicts an excess of dark halos compared to observations. The excess is seen from the estimates of the virialized mass inside the Local Supercluster and its surroundings. It is shown that it is possible to eliminate this contradiction remaining within the framework of the ΛCDM cosmology. This is possible if allowance is made for cosmological velocity fluctuations during the process of formation of the population of dark halos. Based on the formalism of Press and Schechter a model is suggested which allows a quantitative explanation for the observable deficit of the virialized mass in the local Universe.

Keywords: Dark matter – large-scale structure of Universe – galaxies: halos – galaxies: statistics

1 Introduction

There are inconsistencies between the predictions of the ΛCDM cosmological model and the observations concerning the distribution of matter on the scales smaller than the scale of homogeneity of the Universe. In particular, note the deficit of virialized matter in the local Universe (Makarov & Karachentsev, 2011). Counts of the mass of the galaxies, virialized groups, and clusters of galaxies in the Local Supercluster and its environs performed by many authors revealed the lack of mass inside the virialized objects, amounting to a half of an order of magnitude (see the references in Makarov & Karachentsev (2011)). According to the Makarov & Karachentsev (2011) catalog the estimate of the local density parameter inside a sphere of the radius 48 Mpc is about 0.08 ± 0.02. As a possible explanation of this deficit Makarov & Karachentsev (2011) suggested that about 2/3 of matter is located outside the virialized areas. Instead, this dark matter is either concentrated in dark clumps, outside the virial regions, or distributed diffusively. In favor of the idea of dark clumps are observational data on weak lensing (Jee et al., 2005) and disturbed galaxies (Karachentsev et al., 2006).

*Email: kurbatov@inasan.ru

In the formation process of the dark halos population the environment effects, which can lead to the loss of the halo mass or to the ejection of the sub-halos from the parent clusters, have an essential importance. In the numerical model of Diemand et al. (2007) it was shown that the most intensive loss of sub-halo happens before virialization of the parental halo. An already formed halo can accumulate up to 20% of its mass by the accretion of surrounding dark matter.

The environment effects are not the only ones which are able to influence the halo population however. For instance, Valageas (2012) has shown that the velocity fluctuations in dark matter (the author considered the Warm Dark Matter model, WDM) can affect the density fluctuations statistics on scales $\lesssim 0.1\ \mathrm{h}^{-1}$ Mpc. Valageas (2012) did not find any considerable effect of the velocity fluctuations for the dark halos population. It should be emphasized however that the calculations were constrained to corrections to the power spectrum only. Moreover, the approach used in the latter study required modification of the ΛCDM model.

An interesting problem is the possibility of a direct kinematic effect of velocity fluctuations on the process of the formation of individual halos as well as their population. It is well known that velocity fluctuations grow along with density fluctuations (Crocce & Scoccimarro, 2006). Due to the moment conservation, the halo during the formation process inherits the velocity of dark matter averaged over its scale. When this halo becomes involved in the formation process of the larger scale gravitational condensation, its velocity may be large enough to leave the parental structure. This effect may change the history of evolution of dark halos, the dark halos population itself, as well as the history of the chemical evolution of the galaxies.

In this paper a method for accounting for the kinematic effects during the dark halos population process is shortly reported. The evolutionary model is formulated based on the Excursion-Set theory (Bond et al., 1991; Lacey & Cole, 1993) in terms of kinetic equation. A detailed description of the model is given by Kurbatov (2015).

In Section 2 the EPS model is briefly examined. In Section 3 the formation model for an individual halo with kinematic effects is suggested and the kinetic equation for the mass function is obtained. In Section 4 the model is applied to the problem of the virialized mass deficit in the local Universe. Conclusions are presented in Section 5.

2 Formation of the halo population in the EPS model

2.1 Growth of the cosmological perturbations

In the ΛCDM model the Large-Scale Structure of the Universe is formed from the growing fluctuations of density and velocity in the cold dark matter. Evolution law of the structures with characteristic mass m can be linked to the properties of the overdensity field $\delta \equiv (\rho - \rho_{\mathrm{cr},0})/\rho_{\mathrm{cr},0}$, and of the velocity divergence field $\theta \equiv \nabla_{\mathbf{x}}(a\dot{\mathbf{x}})$, averaged over the volume containing mass m. The averaging is defined as a convolution of the field with a filter W. E.g. for the overdensity in the Fourier space*:

$$\tilde{\delta}(a, \mathbf{k}, m) = (2\pi)^{3/2}\, \tilde{W}(\mathbf{k}, m)\, \tilde{\delta}(a, \mathbf{k})\ . \tag{1}$$

*The Fourier transform is defined as $\tilde{f}(\mathbf{k}) = (2\pi)^{-3/2} \int d^3x\, e^{i\mathbf{kx}} f(\mathbf{x})$.

where a is the scale factor. The "top-hat" filter will be adopted for W hereinafter. We will make standard assumptions on the fluctuations fields: they are gaussian, delta-correlated in Fourier space, and undergo linear growth law. The overdensity variance is

$$S(m) = \int d^3k \, |\tilde{W}(\mathbf{k}, m)|^2 \, P(k) \, , \tag{2}$$

where P is the overdensity power spectrum. Let us assume that the high-redshift values of the overdensity and velocity divergence perturbations are proportional to each other. In this case the power spectra of the fields $\tilde{\delta}_{\rm L}(\mathbf{k})$ and $\tilde{\theta}_{\rm L}(\mathbf{k})$ coincide. Denote as $P_v(k) \equiv \langle |\tilde{v}_j(\mathbf{k})|^2 \rangle$ the power spectrum of the velocity in the given spatial direction j (is is assumed to be isotropic) then obtain the velocity power spectrum:

$$P_v(k) = \frac{P_\theta(k)}{k^2} \, . \tag{3}$$

The same as (4) expression is true for the variance of the velocity divergence.

At large redshifts the overdensity and velocity divergence amplitudes evolve according to the linear law (Peebles, 1980; Crocce & Scoccimarro, 2006):

$$P(a,k) = D^2(a) P(k) \, , \qquad S(a,m) = D^2 S(m) \, , \tag{4}$$

$$P_v(a,k) = D_v^2(a) P_v(k) \, , \qquad S_v(a,m) = D_v^2 S_v(m) \, , \tag{5}$$

$$D_v \equiv aHfD \, , \tag{6}$$

where $D = D(a)$ is the linear growth factor; $H = H(a)$ is the Hubble parameter; $f \equiv d \ln D / d \ln a$.

Due to the momentum conservation, the forming halo as a whole inherits the velocity of the proto-halo matter, i.e. the velocity, averaged over proto-halo mass scale. Let us assume that a proto-halo with mass M had velocity $\mathbf{V}(a, \mathbf{X}, M)$. Then the variance of a sub-halo with the mass m, to the first approximation, will depend neither on the position of the sub-halo inside the proto-halo nor the velocity of the proto-halo, but only on the variance of the velocity field on the scale[†] M:

$$S_v(a, m, M) \equiv D_v^2 \left[S_v(m) - S_v(M) \right] . \tag{7}$$

In the present paper the ΛCDM model parameters obtained by the Planck mission Planck Collaboration et al. (2013) were adopted: $h = 0.673$, $\Omega_{\rm m,0} = 0.315$, $\Omega_{\Lambda,0} = 1 - \Omega_{\rm m,0} = 0.685$, $\sigma_8 = 0.828$, $n_{\rm S} = 0.9603$. The power spectrum of the overdensity fluctuations was calculated for these parameters by means of the code CAMB (Lewis et al., 2000) for wavenumbers from 10^{-3} Mpc^{-1} to 2 Mpc^{-1}. Outside of this range, the theoretical power spectrum was used with the power index $n_{\rm S}$ and the transfer function (Bardeen et al., 1986, p. 60) with the shape parameter $\Gamma \equiv h^2 \Omega_{\rm m,0} = 0.14$ Mpc^{-1}. The linear growth factor was adopted from Bildhauer et al. (1992) using normalization $D(a \approx 0) = a$.

[†]The closer the centers of the volumes M and m are to each other, the better this approximation is (Hoffman & Ribak, 1991). See also Kurbatov (2014).

2.2 Evolution of the mass function

The ideas that the EPS model (Peacock & Heavens, 1990; Bond et al., 1991) is based on may be represented as a typical problem of theory of the stochastic processes. A stochastic process $\delta(S)$ starts from the point $\delta = 0$ with the parameter $S = 0$, which corresponds to $m = \infty$. Its evolution obeys equation

$$\frac{d\delta}{dS} = \eta \,, \tag{8}$$

where $\eta = \eta(S)$ is a Gaussian random process with zero mean, unit variance, and the correlation function $\langle \eta(S)\, \eta(S') \rangle = \delta_{\rm D}(S - S')$ (Maggiore & Riotto, 2010). The mass m corresponding to the value of the parameter S, when a certain threshold $\delta_{\rm c}/D(z)$ is reached by the process $\delta(S)$ for the first "time" S, is interpreted as the mass of the halo virialized by the given redshift z. The distribution function of these masses is the halo mass function sought for.

The value $\delta_{\rm c}$ is the linear amplitude of the spherical overdensity perturbation collapsing at the moment z. In the spherical collapse model (Peebles, 1980) this value reduced to the unit growth factor is approximately 1.686. In our case[‡]

$$\delta_{\rm c} = 1.686\, D(z = 0). \tag{9}$$

The resulting halo mass function can be represented as a probability density (Bond et al., 1991; Lacey & Cole, 1993)

$$f^{(0)}(z, S) = \frac{\omega}{\sqrt{2\pi S^3}} \exp\left(-\frac{\omega^2}{2S}\right) \tag{10}$$

or the cumulative distribution function

$$F^{(0)}(z, < S) = \int_0^S dS'\, f^{(0)}(z, S') = \operatorname{erfc}\left(\frac{\omega}{\sqrt{2S}}\right), \tag{11}$$

where notation $\omega \equiv \delta_{\rm c}/D(z)$ is introduced.

The variance S or the mass of a halo with a largest formation rate at the given redshift correspond to the maximum of the function $\partial f^{(0)}/\partial\omega$ and thus obeys equation $\omega^2 = (3+\sqrt{6})\, S$. Most of the halos formed per unit time has the variance in the interval $\log S = \log[\omega^2/(3+\sqrt{6})] \pm 0.5$. At large redshifts, the interval can be estimated as

$$S \approx (0.15 \ldots 1.5)\, (z+1)^2 \,. \tag{12}$$

3 Kinematic effects in the dark matter

3.1 Formation of a single halo

Transition of a spherical perturbation into a halo proceeds in four stages: initial expansion, detachment from the Hubble flow, compression, virialization (Peebles,

[‡]In models of the EPS class the linear growth factor D is usually normalized to take unit value at $z = 0$ (Lacey & Cole, 1993). In the present paper the alternative normalization is used: $D(z) \approx 1/(z+1)$ at $z \gg 1$. For cosmological parameters adopted here (see the previous section) we have $D(z = 0) \approx 0.788$.

1980). The moment of detachment or turnaround point is located approximately in the middle between the start of the expansion and the virialization, when the formation is completed (Peebles, 1980). In the spherical collapse model, the halo formation is described by motion of disjoint layers or test particles in the gravitational field of a point mass. At that, the mass enclosed inside the layer is conserved. For the perturbation to become collapsed at a given redshift $z_{\rm f}$, its linear overdensity must grow as (Lacey & Cole, 1993)

$$\Delta(z) = \frac{D(z)}{D(z_{\rm f})}\,\frac{\delta_{\rm c}}{D(z=0)}\ . \tag{13}$$

It was mentioned above that sub-halos have random velocities relative to the parent halo. Let us consider the possibility that the velocity of the sub-halo is large enough to leave the proto-halo. Let us write an expression for mechanical energy of a test particle inside the parent proto-halo using physical coordinates, and neglecting the Λ-term:

$$E = \frac{\dot{\mathbf{r}}^2}{2} + \Phi\ . \tag{14}$$

At large redshifts, the overdensity amplitude of the parent proto-halo is low, thus the density distribution inside the parent proto-halo may be considered as uniform. Gravitational potential in this case is

$$\Phi = -\frac{GM}{R}\left(\frac{3}{2} - \frac{r^2}{2R^2}\right), \tag{15}$$

where M is the proto-halo mass; the scale R is defined as a physical radius of the proto-halo at the turnaround, containing the mass M:

$$M = \frac{4\pi}{3}\,\rho_{\rm cr,0}\Omega_{\rm m,0}\,(1+\Delta)\,\frac{R^3}{a^3}\ . \tag{16}$$

We formulate the escape condition for the particle as the constraints for the energy value, $E > 0$:

$$(a\dot{x} + aHx)^2 > \frac{H_0^2\Omega_{\rm m,0}}{a}X^2\,(1+\Delta)\left(\frac{3}{2} - \frac{x^2}{2X^2}\right), \tag{17}$$

where $X = R/a$, $x = r/a$, $x \leqslant X$, $a < a_{\rm f}$. Condition (17) defines the lower bound of the velocity sufficient to leave the proto-halo:

$$\dot{x} > -Hx + \left[\frac{H_0^2\Omega_{\rm m,0}}{a^3}\,X^2\,(1+\Delta)\left(\frac{3}{2} - \frac{x^2}{2X^2}\right)\right]^{1/2}. \tag{18}$$

It can be shown (Kurbatov, 2015) that in the high redshift limit, where the low-mass halos form, the sub-halo escape does not affect the formation of the dark halo population.

Let us denote as $\sigma_v \equiv [S_v(m) - S_v(M)]^{1/2}$ the standard deviation of the 1-D velocity (reduced to the unit growth factor) of a sub-halo m relative to a proto-halo

M. The probability for modulus of the Gaussian distributed sub-halo velocity to exceed some v is

$$P_v(>v) = \mathrm{erfc}\left(\frac{v}{\sqrt{2}\,\sigma_v}\right) + \frac{2}{\sqrt{\pi}}\,\frac{v}{\sqrt{2}\,\sigma_v}\,\exp\left(-\frac{v^2}{2\sigma_v^2}\right) . \tag{19}$$

Given the uniform spatial distribution of the sub-halos at the early stage of the proto-halo evolution, the probability for sub-halo m to escape proto-halo M formed at the redshift z_f is

$$\chi_\mathrm{ej}(z_\mathrm{f}, M, m) \equiv \frac{3}{X^3}\int_0^X dx\, x^2 P_v(>v_\mathrm{ej}) , \tag{20}$$

where a threshold velocity value v_ej is the r.h.s. of (18) reduced to the unit growth factor:

$$v_\mathrm{ej} = -\frac{aH}{D_v}\,x + \left[\frac{H_0^2\Omega_{\mathrm{m},0}}{aD_v^2}\,X^2\,(1+\Delta)\left(\frac{3}{2} - \frac{x^2}{2X^2}\right)\right]^{1/2} . \tag{21}$$

Distribution of χ_ej for sub-halos the masses of which are one-third of the parent proto-halo mass is shown in Fig. 1. Comparing the position of contour lines and the mass interval of proto-halos formed by a given era (the mass interval is bounded by thick dashed lines), one can see that for the formation redshifts $z_\mathrm{f} \lesssim 100$ the mass fraction of escaping sub-halos of low masses is approximately constant for all z_f and can be estimated as 15%, roughly. Thereby, a significant fraction of the sub-halos can escape the parent proto-halo, thus avoiding the absorption.

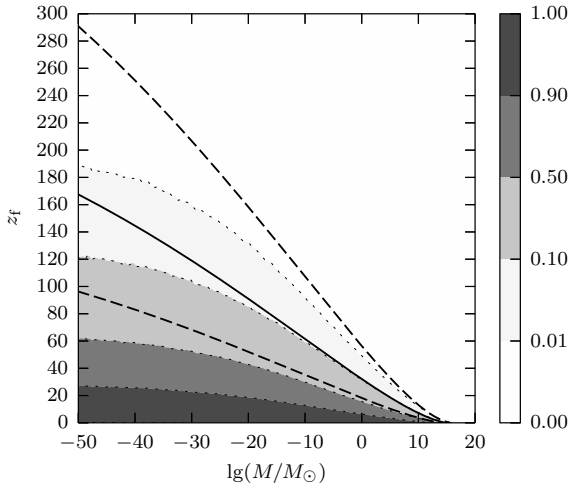


Figure 1 Isolines of the probability of ejection of sub-halos as a function of proto-halo mass (horizontal axis) and redshift (vertical axis). The sub-halo masses are one-third of the proto-halo mass. The solid curve marks the era of the most intensive formation proto-halo of a given mass. The primary mass interval of the proto-halos formed at a given epoch is bounded by the dashed lines.

3.2 Evolution of the mass function with account for kinematic effects

In the standard excursion set approach a mass inside each collapsed perturbation is conserved during the collapse and equals to the subsequent halo mass. This suggestion makes realizations of the random process $\delta(S)$ independent up to some small corrections noted above. As it became clear, proto-halos may lose a significant fraction of the sub-halos resulting in transition of the sub-halos to proto-halo of larger scales which undergo collapse at later times. Consequently, the values of $\delta(S)$ will correlate both in scales and redshifts. This fact makes it difficult to use the excursion set formalism explicitly.

Greater clarity can have an approach based on the kinetic equation, when the evolution of the mass function is explicitly presented as a result of the absorption process of the sub-halo by the large-scale perturbations. The paper by Kurbatov (2015) shows that the kinetic equation which is equivalent to the EPS formalism is

$$-\frac{\partial f^{(0)}(\omega,S)}{\partial\omega} = \\ = \lim_{\Delta\omega\to 0+}\frac{1}{\Delta\omega}\left[\int_S^\infty dS'\, f^{(0)}(\omega,S\,|\,\omega+\Delta\omega,S')\, f^{(0)}(\omega+\Delta\omega,S') - \right. \\ \left. - f^{(0)}(\omega+\Delta\omega,S)\int_0^S dS'\, f^{(0)}(\omega,S'\,|\,\omega+\Delta\omega,S)\right]. \quad (22)$$

This equation has well-defined source and sink and "transfer cross section", which is the conditional PDF $f^{(0)}(\omega,S\,|\,\omega+\Delta\omega,S')$. The latter was obtained by Lacey & Cole (1993) on the ground of markivianity of the random process $\delta(S)$.

It is possible to modify the source and the sink of (22) in a way to allow the mass ejection from the forming halos. After all calculations the kinetic equation has the form (Kurbatov, 2015):

$$-\frac{\partial f}{\partial\omega} = \lim_{\Delta\omega\to 0+}\frac{1}{\Delta\omega}\left[P_+ - P_-\right], \quad (23)$$

where

$$P_+(\omega+\Delta\omega,\omega,S) = \int_S^\infty dS'\,[1-\chi_{\rm ej}(\omega,S,S')]\times \\ \times\, f^{(0)}(\omega,S\,|\,\omega+\Delta\omega,S')\, f(\omega+\Delta\omega,S'), \quad (24)$$

$$P_-(\omega+\Delta\omega,\omega,S) = f(\omega+\Delta\omega,S)\times \\ \times\int_0^S dS''\,[1-\chi_{\rm ej}(\omega,S'',S)]\, f^{(0)}(\omega,S''\,|\,\omega+\Delta\omega,S). \quad (25)$$

Examples of how the sub-halo ejection affects the halo mass function are shown in Fig. 2. In these calculations, the escape probability was assumed constant. Also the EPS mass function was used as the initial PDF. It is clearly seen that for larger escape probability $\chi_{\rm ej}$ the "tail" of the low mass end (high S values) of the mass function becomes heavier , i.e. the evolution of the population effectively slows down as $\chi_{\rm ej}$ increases.

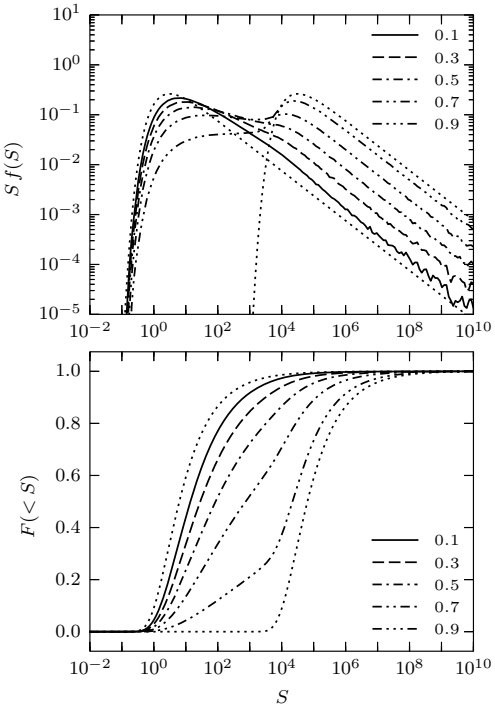


Figure 2 The mass function (PDF and the cumulative) for the case $\chi_{\rm ej} \equiv$ const. The rightmost dashed line designates the initial distribution at $z = 100$ for all runs. The leftmost dashed line designates the final distribution $z = 0$) for the case $\chi_{\rm ej} = 0$. The intermediate curves correspond to various $\chi_{\rm ej}$ (see the legend on the plot).

4 Virialized matter in the local Universe

According to the catalog (Makarov & Karachentsev (2011)), the local density parameter of matter

$$\Omega_{\rm m} \equiv \frac{3M_{\rm m,tot}}{4\pi\rho_{\rm cr,0}D^3}\ , \tag{26}$$

may be estimated as[§] $\Omega_{\rm m} = 0.068 \pm 0.017 = (0.22 \pm 0.05)\Omega_{\rm m,0}$. Here $M_{\rm m,tot}$ is the total mass of matter inside a sphere of radius D. The authors of the catalog proposed several explanations of such a dramatic deficiency. The most plausible of them is the suggested possibility that about 2/3 of dark matter in the Universe is scattered outside the virial or collapsing regions, being distributed diffusively or concentrated in dark "clumps". Indeed, certain evidence for existence of the dark clumps may be provided by the observations of weak lensing events (Natarajan & Springel, 2004; Jee et al., 2005), and the properties of the disturbed dwarf galaxies (Karachentsev et al., 2006).

[§]Original author's value $\Omega_{\rm m} = 0.08 \pm 0.02$ is corrected according to the data of the Planck Collaboration et al. (2013).

The claims of Makarov & Karachentsev (2011) were based on observational data of the virialized groups having masses above $\approx 3 \times 10^{10} M_\odot$, and containing at least two galaxies. Completeness of the sample was 82%. The mass distribution function of the virialized groups (see Fig. 8 in Makarov & Karachentsev (2011)) showed a decrease in the number of objects with masses lower than $10^{13} M_\odot$. This can be caused by the absence of the field galaxies in the sample. In our further analysis we will use just a fraction of the sample composed by the objects as massive as $10^{13} M_\odot$ and above. The reason is that this fraction should more closely match the mass distribution of the dark matter gravitational condensations.

According to EPS distribution, the total mass fraction of the dark matter halos more massive than $10^{13} M_\odot$ is $M_{\rm m}(> 10^{13} M_\odot)/M_{\rm m,tot} \approx 0.27$, i.e. more than 2/3 of all the dark matter settles in the halos with masses below $10^{13} M_\odot$ (see Fig. 3). The observational data (thick solid line on Fig. 3) show the deficit of the virialized halos, up to the factor two and a half in comparison with the EPS prediction: $M_{\rm m}(> 10^{13} M_\odot)/M_{\rm m,tot} \approx 0.11$.

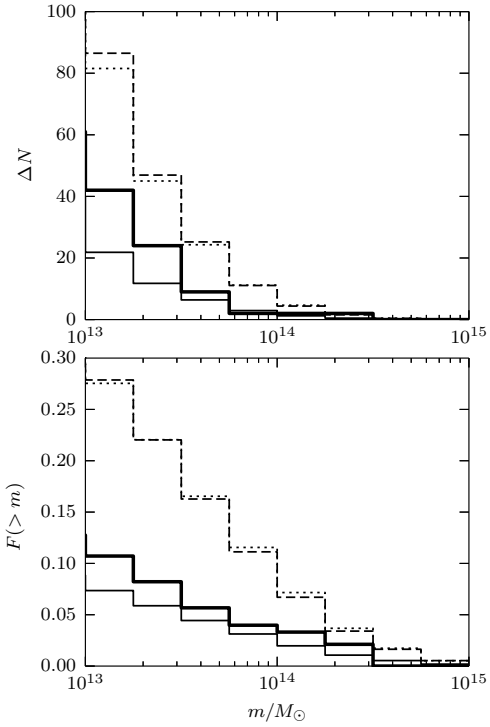


Figure 3 Mass function of the virialized structures with masses $> 10^{13} M_\odot$: the data of Makarov & Karachentsev (2011) (thick solid line), the model with sub-halo ejection (thin solid line), the PS model (dotted line), the PS-like model with alternative initial conditions (dashed line, see Kurbatov (2015)).

Accounting for the effect of sub-halos escape process in the presented model gives the cumulative fraction of all the massive halos about 0.08, i.e. slightly lower than observed. Quite a good agreement between the observed and the theoretical distri-

bution functions of the massive halos is mainly due to the fact that the differential distribution functions for both cases nearly coincide at the masses from $3 \times 10^{13} M_{\odot}$ and above (see the upper plot in Fig. 3), whereas two left bins on this plot show twice as large deficit of the halos predicted the theoretical model suggested in this study. While the uncertainties in the estimates of the groups' masses can be as high as 20% (Makarov & Karachentsev, 2011), the average values of the observed mass function are systematically higher than those of the theoretical one. This may be explained in two ways:

(i) Average matter density in the vicinities of the local Supercluster seems to be higher than cosmological value (Makarov & Karachentsev, 2011). As a consequence of this, the massive tail of the halo mass PDF should be heavier (Mo & White, 1996; Kurbatov, 2014).

(ii) The proposed effect of the mass decrease of proto-halos may be overestimated as we did not account for, e.g., accretion of the matter on the proto-halo from its environment. Diemand et al. (2007) have shown that halos may accrete up to 20% of mass after virialization has ended, i,e., accretion may partially compensate the escape process leading to effective decrease of the escape probability $\chi_{\rm ej}$.

In general, a good agreement between the observed mass function (Makarov & Karachentsev, 2011) and predictions of the model proposed in this paper should be noted.

5 Conclusions

In the present paper the influence of the dark matter random velocities on formation of the dark halos population is considered. It is shown that this kinematic effect leads to the escape of the significant fraction of sub-halos (up to tens of percent). However, at the redshifts greater than 250 the escape is negligible. At moderate and small redshifts the escape probability is higher for sub-halos of lower masses.

We suggested a model of the dark halo population formation, based on the EPS theory. The model was built within the framework of the kinetic approach where the source and sink explicitly describe the hierarchical merging process and the kinematic effects, and potentially may be used to account for environmental effects. The consequences of the sub-halo escape is the redistribution of the massive halos toward lower masses. If no escape is included, the EPS mass function is the invariant solution of the kinetic equation.

The model developed in this paper allowed us to explain quantitatively the observable deficit of the virialized objects in the Local Universe, at least for groups of galaxies with masses greater than $10^{13} M_{\odot}$. The calculations showed that the missing matter is distributed over the low-mass halos.

References

Bardeen, J.M., Bond, J.R., Kaiser, N., & Szalay, A.S. (1986). ApJ, 304, 15–61.
Bildhauer, S., Buchert, T., & Kasai, M. (1992). AAP, 263, 23–29.
Bond, J.R., Cole, S., Efstathiou, G., & Kaiser, N. (1991). ApJ, 379, 440–460.
Crocce, M. & Scoccimarro, R. (2006). Phys. Rev. D, 73(6), 063519–+.
Diemand, J., Kuhlen, M., & Madau, P. (2007). ApJ, 667, 859–877.
Hoffman, Y. & Ribak, E. (1991). ApJL, 380, L5–L8.
Jee, M.J., White, R.L., Benítez, N. & et al. (2005). ApJ, 618, 46–67.
Karachentsev, I.D., Karachentseva, V.E., & Huchtmeier, W.K. (2006). AAP, 451, 817–820.
Kurbatov, E.P. (2014). Astron. Rep., 58, 386–398.
Kurbatov, E.P. (2015). Astron. Rep., 59, 257–270.
Lacey, C. & Cole, S. (1993). MNRAS, 262, 627–649.
Lewis, A., Challinor, A., & Lasenby, A. (2000). ApJ, 538, 473–476.
Maggiore, M. & Riotto, A. (2010). ApJ, 711, 907–927.
Makarov, D. & Karachentsev, I. (2011). MNRAS, 412, 2498–2520.
Mo, H.J. & White, S.D.M. (1996). MNRAS, 282, 347–361.
Natarajan, P. & Springel, V. (2004). ApJL, 617, L13–L16.
Peacock, J.A. & Heavens, A.F. (1990). MNRAS, 243, 133–143.
Peebles, P.J.E. (1980). The large-scale structure of the universe. Princeton, N.J.: Princeton Univ. Press.
Planck Collaboration, Ade, P.A.R., Aghanim, N., Armitage-Caplan, C., Arnaud, M. et al. (2013). ArXiv:1303.5076.
Valageas, P. (2012). Phys. Rev. D, 86(12), 123501.